

# First Octameric Ellipsoid Lanthanide(III) Complexes: Crystal Structure and Nonlinear Optical Absorptive and Refractive Properties

Hongwei Hou,<sup>\*,†</sup> Yongli Wei,<sup>†</sup> Yinglin Song,<sup>‡</sup> Yaoting Fan,<sup>†</sup> and Yu Zhu<sup>†</sup>

Department of Chemistry, Zhengzhou University, Henan 450052, P. R. China, and Department of Applied Physics, Harbin Institute of Technology, Heilongjiang 150001, P. R. China

Received October 28, 2003

The ligand *N,N'*-bis(1,3,4-thiazolyl)-2,6-pyridyldicarboxamide (btapca) has been synthesized and its coordination properties toward La(III) and Ce(III) in the presence of air have been investigated. The complexes  $[\text{Ln}_8(\text{tbzcapc})_{12}(\text{H}_2\text{O})_{24}] \cdot 6\text{DMF}$  ( $\text{Ln} = \text{La}$ , **1**,  $\text{Ce}$ , **2**;  $\text{tbzcapc} = 6\text{-}[2\text{-}N\text{-}(1,3,4\text{-thiazolyl})\text{carboxamido}]\text{-2-pyridylcarboxylate}$ ) show octameric ellipsoid structures. We found the starting ligand btapca had been altered into tbzcapc during the formation process of  $[\text{Ln}_8(\text{tbzcapc})_{12}(\text{H}_2\text{O})_{24}] \cdot 6\text{DMF}$ . The NLO properties of complexes **1** and **2** were investigated via Z-scan techniques. It is interesting that the two isostructural complexes show completely different NLO properties. Complex **1** shows NLO refractive effects without absorption, while complex **2** possesses NLO absorptive behavior without refraction.

## Introduction

Coordination chemistry has undergone a great proliferation in recent years. Especially, the assembly of sophisticated high-nuclearity coordination complexes with lanthanide(III) ions attracts much more attention.<sup>1–5</sup> By now, a host of fascinating lanthanide-based supramolecular architectures have been reported such as a hexameric europium wheel,<sup>5</sup> trinuclear lanthanide complexes,<sup>1</sup> samarium macrocyclic clusters,<sup>6</sup> and a three-dimensional cylinder.<sup>7</sup>

However, while the number of polynuclear lanthanide coordination compounds is rapidly increasing, the assembly of this kind of supramolecular architecture is still limited to certain degree, because the trivalent lanthanide ions show little stereochemical preferences,<sup>2,5,8,9</sup> which generally display high and variable coordination numbers. These factors related

to lanthanide(III) ions lagged the design of the construction of lanthanide superlattices. But taking advantage of many factors including favorable symmetry and entropy effects, preprogrammability of the building blocks, and sometimes the reversibility of metal–ligand ligation, assembly from well-chosen lanthanide ions and multidentate ligands becomes much accessible.<sup>10–12</sup> In recent years, polynuclear lanthanide–hydroxo complexes have received much consideration, and some groups have reported a series of high-nuclearity lanthanide–hydroxo complexes prepared via lanthanide hydrolysis controlled by  $\alpha$ -amino acids as supporting ligands.<sup>13,14</sup>

To amplify the scope of lanthanide coordination complexes, our group focuses much effort on pursuing suitable

\* To whom correspondence should be addressed. E-mail: houhongw@zzu.edu.cn.

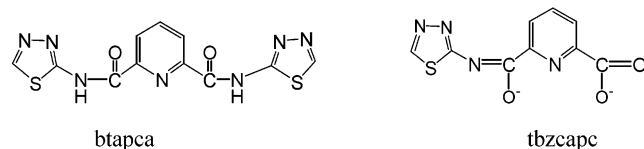
<sup>†</sup> Zhengzhou University.

<sup>‡</sup> Harbin Institute of Technology.

- Brettonnière, Y.; Mazzanti, M.; Wietzke, R.; Pécaut, J. *Chem. Commun.* **2000**, 1543.
- Xu, J.; Raymond, K. N. *Angew. Chem., Int. Ed.* **2000**, *39*, 2745.
- Fatin-Rouge, N.; Tóth, É.; Perret, D.; Backer, R. H.; Merbach, A. E.; Bünzli, J. C. G. *J. Am. Chem. Soc.* **2000**, *122*, 10810.
- Caravan, P.; Comuzzi, C.; Crook, W.; McMurry, T. J.; Choppin, G. R.; Woulfe, S. R. *Inorg. Chem.* **2001**, *40*, 2170.
- Brettonnière, Y.; Mazzanti, M.; Wietzke, R.; Pécaut, J.; Olmstead, M. M. *J. Am. Chem. Soc.* **2002**, *124*, 9012.
- Ganesan, M.; Gambarotta, S.; Yap, G. P. A. *Angew. Chem., Int. Ed.* **2001**, *40*, 766.
- Johnson, D. W.; Xu, J.; Saalfrank, R. W.; Raymond, K. N. *Angew. Chem., Int. Ed.* **1999**, *38*, 2882.

- (8) (a) Kepert, D. *Inorganic Stereochemistry*; Springer: Berlin, Germany, 1982; Chapter 2, pp 12–16. (b) Bünzli, J. C. G. *Basic and Applied Aspects of Rare Earths*; Editorial Complutense: Madrid, 1997.
- (9) Bünzli, J. C. G. *Lanthanides Probes in Life, Chemical and Earth Sciences*; Elsevier: Amsterdam, 1989; Chapter 7.
- (10) Anwender, R. *Angew. Chem., Int. Ed.* **1998**, *37*, 599.
- (11) Lehn, J. M. *Supramolecular Chemistry: Concepts and Perspectives*; VCH: Weinheim, Germany, 1995.
- (12) Cui, Y.; Ngo, H. L.; Lin, W. B. *Inorg. Chem.* **2002**, *41*, 5940.
- (13) (a) Wang, R.; Liu, H.; Carducci, M. D.; Jin, T.; Zheng, C.; Zheng, Z. *Inorg. Chem.* **2001**, *40*, 2743. (b) Wang, R.; Carducci, M. D.; Zheng, Z. *Inorg. Chem.* **2000**, *39*, 1836. (c) Wang, R.; Selby, H. D.; Liu, H.; Carducci, M. D.; Jin, T.; Zheng, Z.; Anthis, J. W.; Staples, R. J. *Inorg. Chem.* **2002**, *41*, 278. (d) Wang, R.; Zheng, Z. *Comments Inorg. Chem.* **2000**, *22*, 1. (e) Wang, R.; Jin, T.; Zheng, Z. *Acta Chim. Sin.* **2000**, *58*, 1481.
- (14) Wang, R.; Jin, T.; Zheng, Z.; Staples, R. J. *Angew. Chem., Int. Ed.* **1999**, *38*, 1813.

Chart 1



ligands to combine with various lanthanide ions in the hunt for superior lanthanide superlattices with novel architectures. Here we report the first octameric ellipsoid lanthanide complexes  $[\text{Ln}_8(\text{tbzcapc})_{12}(\text{H}_2\text{O})_{24}] \cdot 6\text{DMF}$  ( $\text{Ln} = \text{La}$ , **1**,  $\text{Ce}$ , **2**;  $\text{tbzcapc} = 6\text{-}[2\text{-}N\text{-}(1,3,4\text{-thiobiazolyl})\text{carboxamido}]\text{-2-pyridylcarboxylate}$ ), which were got from  $\text{Ln}(\text{III})$  ions reacting with the ligand btapca (Chart 1), and find that they show interesting third-order NLO properties.

## Experimental Section

**General Procedure.** All chemicals were purchased from Aldrich and used as received. A PE 240C elemental analyzer performed carbon, hydrogen, and nitrogen analyses. Fast atom bombardment (FAB) mass spectra were obtained on a Bruker Esquire 3000 mass spectrometer. NMR spectra were obtained using a Bruker DPX-400 spectrometer.

**Synthesis of Ligand  $N,N'$ -Bis(1,3,4-thiobiazolyl)-2,6-pyridyldicarboxamide (btapca).** 2,6-Pyridyldicarboxylic acid (1.67 g, 10 mmol) was directly dissolved in 20 mL of  $\text{SOCl}_2$ . The reaction solution was refluxing until the white powder dissolved completely. And the residue  $\text{SOCl}_2$  was moved away under reduced pressure. The resulting 2,6-pyridinedicarboxylic acid chlorides were dissolved in 10 mL of dry py. Then the py solution of 2-aminobithiazole (2.02 g, 20 mmol) was dropwise added into the 2,6-pyridinedicarboxylic acid chloride under stirring in the ice bath. Continuous stirring for 4 h resulted in white precipitates. The precipitates were filtered out under reduced pressure and were washed by water and methanol, respectively. The dried product weighted 2.25 g (yielding 70%). Anal. Calcd for  $\text{C}_{11}\text{H}_7\text{N}_7\text{O}_2\text{S}_2$ : C, 39.64; H, 2.12; N, 29.41. Found: C, 39.84; H, 2.27; N, 28.11.  $^1\text{H}$  NMR (400 MHz, DMSO):  $\delta = 8.39$  (q, H),  $\delta = 8.50$  (d, 2H),  $\delta = 9.36$  (s, 2H),  $\delta = 13.73$  (d, 2H). Positive-ion ESI-MS:  $m/z$  333.9 [btapca +  $\text{H}^+$ ].

**Synthesis of Octameric  $[\text{Ln}_8(\text{tbzcapc})_{12}(\text{H}_2\text{O})_{24}] \cdot 6\text{DMF}$ .** The reaction of  $\text{Ln}(\text{NO}_3)_3 \cdot 9\text{H}_2\text{O}$  ( $\text{Ln} = \text{La}$ ,  $\text{Ce}$ ) with 0.5 equiv of btapca ( $\text{btapca} = N,N'$ -bis(1,3,4-thiobiazolyl)-2,6-pyridyldicarboxamide) in a solvent of DMF and MeOH resulted in the formation of complexes  $[\text{Ln}_8(\text{tbzcapc})_{12}(\text{H}_2\text{O})_{24}] \cdot 6\text{DMF}$  ( $\text{Ln} = \text{La}$ , **1**,  $\text{Ce}$ , **2**), respectively. Light yellow crystals suitable for X-ray diffraction were obtained 2 months later. Yield: 30% for **1**; 25% for **2**.  $^1\text{H}$  NMR (400 MHz, DMSO): **1**,  $\delta = 7.96$  (d, H),  $\delta = 8.03$  (q, 12H),  $\delta = 8.22$  (d, 5H),  $\delta = 8.40$  (q, H),  $\delta = 8.51$  (d, 2H),  $\delta = 8.74$  (s, 4H),  $\delta = 9.04$  (s, H),  $\delta = 9.36$  (s, H),  $\delta = 13.73$  (s, 2H); **2**,  $\delta = 7.95$  (s, 3H),  $\delta = 9.22$  (s, 2H),  $\delta = 9.71$  (s, 3H),  $\delta = 10.38\text{--}10.90$  (br, 2H),  $\delta = 11.45$  (s, 2H).

**X-ray Crystallographic Analysis.** X-ray diffraction results indicate that **1** and **2** are isostructural. The diffraction intensities of prismatic crystals of complexes **1** and **2** were collected with graphite-monochromatized Mo  $\text{K}\alpha$  X-radiation ( $\lambda = 0.71073 \text{ \AA}$ ) using a Shimadzu R-AXIS-IV diffractometer at 291(2) K to a maximum  $2\theta$  value of  $50^\circ$ . The unit cell parameters were determined from the reflections collected on oscillation frames and were then refined. The data were corrected for Lorentz and polarization effects. The structures were solved by direct methods with SHELXS-97<sup>15</sup> and subsequent Fourier-difference synthesis and

Table 1. Crystallographic Data

	1	2
formula	$\text{C}_{126}\text{H}_{138}\text{La}_8\text{N}_{54}\text{O}_{66}\text{S}_{12}$	$\text{C}_{126}\text{H}_{138}\text{Ce}_8\text{N}_{54}\text{O}_{66}\text{S}_{12}$
fw	4960.90	4970.58
space group	$R\bar{3}$	$R\bar{3}$
$a$ , $\text{\AA}$	26.731(4)	26.680(4)
$b$ , $\text{\AA}$	26.731(4)	26.680(4)
$c$ , $\text{\AA}$	21.435(4)	21.388(4)
$\gamma$ , deg	120	120
$V$ , $\text{\AA}^3$	13 264(4)	13 185(4)
$Z$	3	3
$D_{\text{calcd}}$ , $\text{g}\cdot\text{cm}^{-3}$	1.863	1.878
$T$ , K	291(2)	291(2)
$\mu$ , $\text{cm}^{-1}$	2.133	2.274
$2\theta_{\text{max}}$ , deg	50	50
reflens measd	11 555	11 566
reflens used ( $R_{\text{int}}$ )	4548	4547
params	376	376
final R vales	$R1 = 0.0786^a$	$R1 = 0.0686^a$
[ $I > 2\sigma(I)$ ]	$wR2 = 0.2055^b$	$wR2 = 0.1717^b$
R values (all data)	$R1 = 0.0971^a$	$R1 = 0.0863^a$
	$wR2 = 0.2168^b$	$wR2 = 0.1808^b$
GOF on $F^2$	1.122	1.086

<sup>a</sup>  $R1 = \sum ||F_o| - |F_c|| / \sum |F_o|$ . <sup>b</sup>  $wR2 = \{ \sum [w(F_o^2 - F_c^2)^2 / \sum [w(F_o^2)^2] ]^{1/2}$ ,  $w = 1 / [\sigma^2(F_o^2) + (0.0786P)^2 + 298.64P]$ , where  $P = (\max(F_o^2, 0) + 2F_c^2) / 3$ .

refined by the full-matrix least-squares method on  $F^2$  with SHELXL-97.<sup>16</sup> All non-hydrogen atoms except atoms in disordered parts were refined anisotropically, and hydrogen atoms were placed at calculated positions and refined as riding atoms with isotropic displacement parameters. Crystal data and structure refinement details for the two compounds are given in Table 1.

**Nonlinear Optical Measurements.** DMF solutions of complexes **1** and **2** were placed in 1 mm quartz cuvettes for NLO measurements. The nonlinear refraction was measured with linearly polarized laser light ( $\lambda = 532 \text{ nm}$ ; pulse widths = 7 ns) generated from a Q-switched and frequency-doubled Nd:YAG laser. The spatial profiles of the optical pulses were nearly Gaussian. The laser beam was focused with a 25-cm focal-length focusing mirror. The radius of the beam waist was measured to be  $35 \pm 5 \mu\text{m}$  (half-width at  $1/e^2$  maximum). The interval between the laser pulses was chosen to be  $\sim 5 \text{ s}$  for operational convenience. The incident and transmitted pulse energies were measured simultaneously by two Laser Precision detectors (RJP-735 energy probes), which were linked to a computer by an IEEE interface. The NLO properties of the samples were manifested by moving the samples along the axis of the incident beam ( $Z$ -direction) with respect to the focal point.<sup>17</sup> An aperture of 0.5 mm in radius was placed in front of the detector to assist the measurement of the self-focusing effect.

## Results and Discussion

**Synthesis of  $[\text{Ln}_8(\text{tbzcapc})_{12}(\text{H}_2\text{O})_{24}] \cdot 6\text{DMF}$  ( $\text{Ln} = \text{La}$ , **1**,  $\text{Ce}$ , **2**).** We found that the starting ligand btapca changed to tbzcapc in the forming process of **1** and **2**. On the contrary, btapca showed great stability in the presence “first-row” transition metals and also formed polynuclear complexes with special structures.<sup>18</sup> This is probably because La and Ce ions induce the activation and cleavage of the carboxamido bond.

(15) Sheldrick, G. M. *Acta Crystallogr., Sect. A* **1990**, *46*, 467.

(16) Sheldrick, G. M. *SHELXL-97, Program for the Refinement of Crystal Structures*; University of Göttingen: Göttingen, Germany, 1997.

(17) (a) Sheik-Bahae, M.; Said, A. A.; Wei, T. H.; Hagan, D. J.; Stryland, E. W. V. *IEEE J. Quantum Electron.* **1990**, *26*, 760. (b) Hou, H. W.; Xin, X. Q.; Liu, J.; Chen, M. Q.; Shi, S. J. *Chem. Soc., Dalton Trans.* **1994**, 3211.

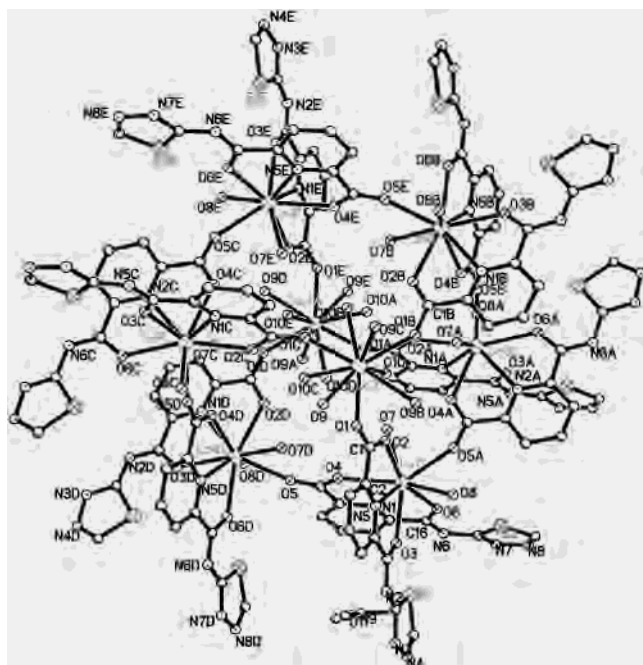


**Figure 1.** Crystal structure of discrete neutral unit  $[\text{La}_8(\text{tbzcapc})_{12}(\text{H}_2\text{O})_{24}]$  with thermal ellipsoids at 30% probability.

High coordination numbers of lanthanide elements have advantages in certain organic reactions that can be promoted catalytically in the presence of lanthanide ions.<sup>19</sup> The catalytic roles of lanthanide ions and their complexes in the hydrolytic cleavage of phosphate diesters have been considerably studied.<sup>13a</sup> However, so far, the identification of the catalytic mechanism has not been ambiguously rendered.<sup>13a</sup> In this paper, the ligand btapca has been changed to tbzcapc in the presence of  $\text{Ln}^{\text{III}}$  ions.

**Crystal Structure of  $[\text{Ln}_8(\text{tbzcapc})_{12}(\text{H}_2\text{O})_{24}] \cdot 6\text{DMF}$  ( $\text{Ln} = \text{La}$ , **1**,  $\text{Ce}$ , **2**).** As shown in Figure 1, complex **1**, containing 8 La(III) ions and 12 ligands in addition to the aqua ligands, crystallizes as discrete ellipsoid-shaped units with space between these ellipsoids filled with solvent molecules. Selected bond length and angle data are listed in Table 2. An X-ray crystallographic analysis unambiguously reveals that units of **1** have an ellipsoid structure  $[\text{La}_8(\text{tbzcapc})_{12}(\text{H}_2\text{O})_{24}]$  with idealized  $C_3$  symmetry. Six La(1) ions, each coordinated by three ligands, define the quasi-equatorial plane, while the other two La(2) ions are at the axial positions. The ellipsoid is compressed along the pseudo- $C_3$  axis, with an  $\text{La}(2) \cdots \text{La}(2A)$  distance of 6.876 Å. Not all the La(1) atoms are rigorously coplanar; the  $\text{La}(2) \cdots \text{La}(1)$  distance averages 7.144 Å, while the distance of the adjacent two La(1) atoms around the equator of the ellipsoid is 6.674 Å. Every La atom is connected with other three La atoms through three  $\mu$ -carboxylate groups from three ligands. A space-filling representation of complex **1** clearly indicates the formation of the ellipsoid cage (Figure 2). Taking the distances of  $\text{La}(2) \cdots \text{La}(2A)$  (6.876 Å),  $\text{La}(1) \cdots \text{La}(1E)$  (12.585 Å), and  $\text{La}(1B) \cdots \text{La}(1D)$  (12.585 Å) as three

**Table 2.** Selected Bond Distances (Å) and Angles (deg) of Complexes **1** and **2**

	<b>1</b>	<b>2</b>	<b>2</b>	<b>2</b>
La(1)—O(3)	2.495(7)	Ce(1)—O(3)	2.472(6)	
La(1)—O(6)	2.525(7)	Ce(1)—O(6)	2.511(7)	
La(1)—O(8)	2.609(8)	Ce(1)—O(8)	2.588(7)	
La(1)—O(2)	2.530(8)	Ce(1)—N(5)	2.636(8)	
La(1)—O(4)	2.537(7)	Ce(1)—N(1)	2.644(8)	
La(1)—O(7)	2.639(9)	Ce(1)—O(1)	2.502(7)	
La(1)—N(5)	2.669(8)	Ce(1)—O(4)	2.519(7)	
La(1)—N(1)	2.679(9)	Ce(1)—O(5)	2.466(7)	
La(2)—O(1)	2.418(9)	Ce(2)—O(9)	2.609(14)	
La(2)—O(9)	2.649(15)	Ce(2)—O(2)	2.412(9)	
La(2)—O(10)	2.693(13)	Ce(2)—O(10)	2.670(13)	
O(5) <sup>#1</sup> —La(1)—O(3)	131.5(3)	O(3)—Ce(1)—O(1)	122.7(2)	
O(5) <sup>#1</sup> —La(1)—O(6)	74.5(3)	O(3)—Ce(1)—O(6)	74.3(2)	
O(6)—La(1)—O(2)	159.4(3)	O(1)—Ce(1)—O(6)	158.0(2)	
O(3)—La(1)—O(6)	74.5(2)	O(3)—Ce(1)—O(4)	88.7(2)	
O(3)—La(1)—O(2)	121.3(3)	O(5)—Ce(1)—O(3)	131.5(3)	
O(3)—La(1)—O(4)	88.7(3)	O(5)—Ce(1)—O(1)	83.9(3)	
O(3)—La(1)—N(5)	73.3(2)	O(3)—Ce(1)—N(5)	73.1(2)	
N(5)—La(1)—N(1)	113.6(2)	N(5)—Ce(1)—N(1)	113.9(2)	
O(1)—La(2)—O(1) <sup>#2</sup>	120.000(5)	O(6)—Ce(1)—N(1)	133.1(2)	
O(1)—La(2)—O(1) <sup>#3</sup>	120.000(3)	O(2)—Ce(2)—O(2)	119.991(13)	
O(1)—La(2)—O(9) <sup>#2</sup>	66.9(5)	O(2)—Ce(2)—O(9) <sup>#2</sup>	67.4(5)	
O(1) <sup>#3</sup> —La(2)—O(9) <sup>#2</sup>	139.3(6)	O(2) <sup>#3</sup> —Ce(2)—O(9) <sup>#2</sup>	139.4(6)	
O(1)—La(2)—O(9)	68.5(4)	O(9) <sup>#2</sup> —Ce(2)—O(9)	81.4(9)	
O(9) <sup>#2</sup> —La(2)—O(9)	82.1(8)	O(2)—Ce(2)—O(10)	132.8(4)	
O(1)—La(2)—O(10)	70.6(3)	O(9)—Ce(2)—O(10)	138.7(4)	
O(9) <sup>#2</sup> —La(2)—O(10)	87.4(6)	O(10) <sup>#3</sup> —Ce(2)—O(10)	72.9(5)	

<sup>a</sup> Symmetry transformations used to generate equivalent atoms: (#1)  $x - y + 1/3, x - 1/3, -z + 2/3$ ; (#2)  $-y + 1, x - y, z$ ; (#3)  $-x + y + 1, -x + 1, z$ ; (#4)  $y + 1/3, -x + y + 2/3, -z + 2/3$ .

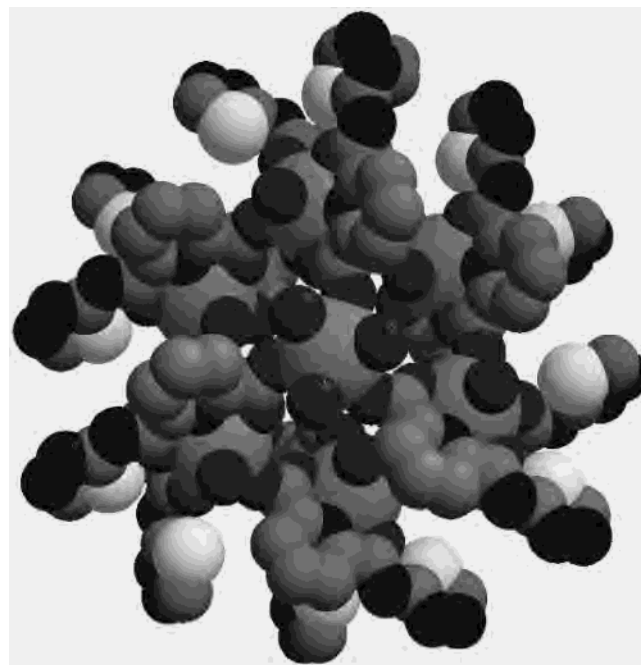


**Figure 2.** Space-filling model of complex **1** as viewed down the [001] direction.

diameters of the ellipsoid for approximation, **1** has a real unoccupied space of  $\sim 638 \text{ \AA}^3$ .

The coordination environments of the La atoms are also noteworthy. Figure 3 describes the coordination modes of the Ln centers. For clarity of description, this species also can be formulated as the cyclic structure  $[(\text{H}_2\text{O})_{12}\text{La}_2(\text{tbzcapc})_{12}\text{La}_6(\text{H}_2\text{O})_{12}]$  in which six  $\text{La}(1)(\text{tbzcapc})_2$  com-

(18) Wei, Y. L.; Hou, H. W.; Zhu, Y.; Fan, Y. T. *Inorg. Chem.*, to be revised.

(19) Mikami, K.; Terada, M.; Matsuzawa, H. *Angew. Chem., Int. Ed.* **2002**, *41*, 3554.

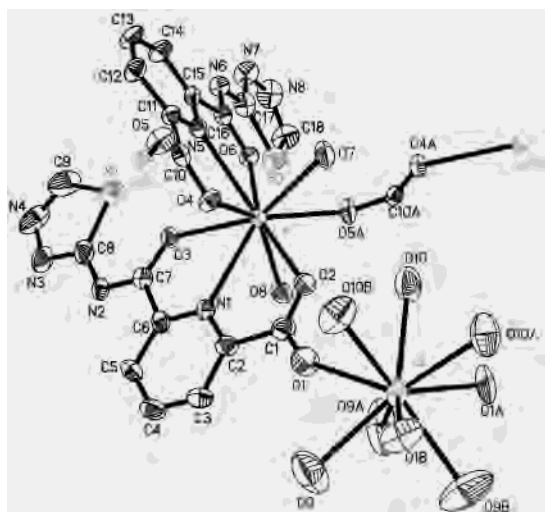


**Figure 3.** Coordination geometries and linkage modes of La atoms.

ponents are connected by six bridging carboxylates to yield a ring encapsulated by two La(2) cations (Figure 1). Both La(1) and La(2) are nine-coordinate. The two possible ground-state geometries for nine-coordination polyhedron are the symmetrical tricapped trigonal prism with  $D_{3h}$  symmetry and the monocapped square antiprism with  $C_{4v}$  symmetry. The polyhedron of the La(1) coordination sphere is best described as a distorted monocapped square antiprism. Each La(1) is coordinated by N(1), N(5), O(2), O(3), O(4), and O(6) from two coordination ligands, O(5A) from another ligand, and another two oxygens O(7) and O(8) from solvent water. The coordination polyhedron of La(2) can be described as a distorted tricapped trigonal prism, which is composed of three oxygens from bridging carboxylate groups and six oxygens from solvent water. Each carboxylate group in the tbzcapc ligand functions as a bridge. Of the two ligands in one La(1)(tbzcapc)<sub>2</sub>, one carboxylate group bridges La(1) and La(2) and the other bridges La(1) and another La(1) atom. The mean La(1)–O distance (2.542 Å) is close to the mean La(2)–O distance (2.587 Å), which is significantly shorter than the mean La(1)–N distance (2.678 Å). These distances are comparable to the corresponding distances in cation [La<sub>3</sub>(μ<sub>3</sub>-treterpy)<sub>2</sub>(OTf)<sub>4</sub>(H<sub>2</sub>O)<sub>2</sub>]<sup>5+</sup>.<sup>1</sup>

The ellipsoid architecture of this species is novel, which is different from preliminary results for Eu<sup>III</sup>,<sup>5,20,21</sup> La<sup>III</sup>, and Sm<sup>II</sup> complexes with ring structures<sup>2,6</sup> and [Ln<sub>4</sub>(μ<sub>3</sub>-OH)<sub>4</sub>]<sup>8+</sup> with a cubanelike core.<sup>13a</sup> In octameric cluster [La<sub>8</sub>L<sup>1</sup>]<sub>8</sub> (L<sup>1</sup> = 4-(1,3,5-benzenetricarbonyl)tris(3-methyl-1-phenyl-2-pyrazolin-5-one)),<sup>2</sup> three bidentate pyrazolone chelating units coordinate eight lanthanum centers resulting in a cyclic lanthanide cluster complexes with a three-dimensional and highly symmetric ring structure. Mazzanti et al. reported a unique wheellike structure [Eu<sub>8</sub>(EuL<sub>2</sub>)<sub>6</sub>]<sup>9+</sup> (HL = 2,2':6',2''-terpyridine-6-carboxylic acid) in which six EuL<sub>2</sub> components are connected by six bridging carboxylates to yield a ring encapsulating an octahedral Eu(III) cation,<sup>5</sup> while [Ln<sub>8</sub>(tbzcapc)<sub>12</sub>(H<sub>2</sub>O)<sub>24</sub>] has an ellipsoid-caged structure. When

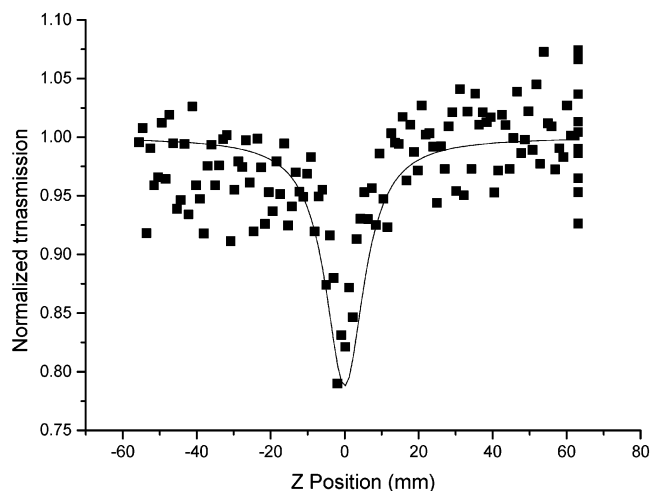


**Figure 4.** Z-scan data for **2** in  $2.0 \times 10^{-4}$  mol dm<sup>-3</sup> DMF solution, obtained under an open aperture configuration. The black dots are the experimental data, and the solids curve is the theoretical fit.

we make a further comparison between the title species and other lanthanide–hydroxo core complexes such as [Ln<sub>15</sub>(μ<sub>3</sub>-OH)<sub>20</sub>(μ<sub>5</sub>-X)]<sup>24+</sup> (Ln = Eu, Nd, Gd, Pr, Eu; X = Cl, Br),<sup>13c</sup> we found there are also some novelties in the title species [Ln<sub>8</sub>(tbzcapc)<sub>12</sub>(H<sub>2</sub>O)<sub>24</sub>]. In the complexes core [Ln<sub>15</sub>(μ<sub>3</sub>-OH)<sub>20</sub>(μ<sub>5</sub>-X)]<sup>24+</sup>, Ln atoms are connected by oxygen atoms and supported by X atoms, while, in [Ln<sub>8</sub>(tbzcapc)<sub>12</sub>(H<sub>2</sub>O)<sub>24</sub>], only oxygens bridge all Ln atoms and tbzcapc acts as a multidentate ligand that utilizes its *N*-pyridyl, carbonyl, and carboxylate groups. The tbzcapc ligand not only triple-coordinates to one Ln atom but also bridges another Ln atom through a carboxylate group. Considering the above two aspects, we feel octanuclear ellipsoid [Ln<sub>8</sub>(tbzcapc)<sub>12</sub>(H<sub>2</sub>O)<sub>24</sub>] is another interesting species.

**Nonlinear Optical Properties.** The third-order NLO properties of complexes **1** and **2** were investigated with 532 nm laser pulses of 7 ns duration by Z-scan experiment in DMF solution. The results show that complex **1** has no NLO absorption but gives strong NLO refractive effects and complex **2** possesses NLO absorptive behavior but no NLO refractive effects.

It should be pointed out that both excited-state population (and absorption) and two-photo absorption can be responsible for the measured NLO effect.<sup>22</sup> The NLO absorption components were evaluated by a Z-scan experiment under an open aperture configuration. The NLO absorption data can be well represented by equations which describe a third-order NLO absorption process.<sup>17a</sup> Figure 4 depicts the NLO absorptive properties of **2**. The figure clearly illustrates that the absorption increases as the incident light irradiance rises since light transmittance (*T*) is a function of the sample's *Z* position. The black dots are the experimental data, and the solids curves are the theoretical fit by using Z-scan theory described in ref 17a. It is obvious that the theoretical curves qualitatively reproduce well the general pattern of observed experimental data. This fact suggests an effective third-order characteristic for experimentally detected NLO effects. The

(20) Pernin, C. G.; Ibers, J. A. *Inorg. Chem.* **1997**, *36*, 3802.

(21) Evans, W. J.; Greci, M. A.; Ziller, J. W. *Inorg. Chem.* **2000**, *39*, 3213.

(22) Ji, W.; Du, H. J.; Shi, S. J. *Opt. Soc. Am.* **1995**, *12*, 876.

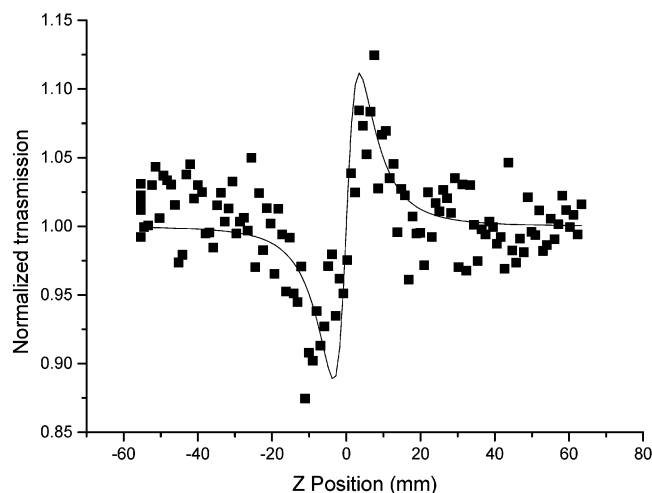


**Figure 5.** Z-scan data for **1** in  $2.0 \times 10^{-4}$  mol dm $^{-3}$  DMF solution, obtained by dividing the normalized Z-scan measured under a closed aperture configuration by the normalized Z-scan data obtained under the open-aperture configuration. The black dots are the experimental data, and the solids curve is the theoretical fit.

nonlinear absorptive index  $a_2$  of **2** is calculated to be  $6.8 \times 10^{-10}$  mW $^{-1}$  in  $2.0 \times 10^{-4}$  mol dm $^{-3}$  DMF solution. The value is better than those for the reported organometallic compounds, semiconductors, and fullerene.<sup>23</sup>

The nonlinear refractive components were assessed by dividing the normalized Z-scan data obtained under the closed aperture configuration by the normalized Z-scan data obtained under the open aperture configuration. Figure 5 presents the typical NLO refractive data for **1**. The data show that **1** has a positive sign for the nonlinear refraction and exhibits strong self-focusing behavior. A reasonably good fit between the experimental data (black dot) and the theoretical curves (solids curves) based on ref 17a was obtained. The effective third-order refractive index  $n_2$  of **1** is calculated to be  $1.4 \times 10^{-11}$  esu.

It is very interesting that the two isostructural complexes show completely different NLO properties. Complex **1** shows NLO refractive effects without NLO absorption, while complex **2** possesses NLO absorptive behavior without NLO refraction.

Many isostructural complexes possess the same NLO properties. We also found some reported isostructural complexes show different NLO properties, but their NLO properties are only changed from self-defocusing to self-focusing such as clusters [MoOS $_3$ Cu $_3$ I(py) $_5$ ] and [WOS $_3$ Cu $_3$ I(py) $_5$ ],<sup>24</sup> the former possesses self-defocusing properties, while the latter exhibits self-focusing properties. Clusters [NEt $_4$ ] $_3$ [MoOS $_3$ (CuBr) $_3(\mu_2$ -Br)]<sup>25</sup> and [NEt $_4$ ] $_3$ [WOS $_3$ (CuBr) $_3(\mu_2$ -Br)]<sup>26</sup> contain different heavy atoms too, and they show self-defocusing and self-focusing effects, respectively. In a comparison of [NEt $_4$ ] $_3$ [WOS $_3$ (CuBr) $_3(\mu_2$ -Br)]<sup>26</sup> with [NEt $_4$ ] $_3$ [WOS $_3$ (CuI) $_3(\mu_2$ -I)],<sup>27</sup> though W atoms exist in the both clusters, different halogen anions (Br or I) lead to the opposite NLO effects; [NEt $_4$ ] $_3$ [WOS $_3$ (CuBr) $_3(\mu_2$ -Br)] exhibits self-focusing, and [NEt $_4$ ] $_3$ [WOS $_3$ (CuI) $_3(\mu_2$ -I)] shows self-defocusing effects. For cluster polymers {[NMe $_4$ ] $_2$ [MoOS $_3$ Cu $_3(\mu_2$ -I) $_3$ ]} $_n$  and {[NMe $_4$ ] $_2$ [WOS $_3$ Cu $_3(\mu_2$ -I) $_3$ ]} $_n$ , {[NMe $_4$ ] $_2$ [MoOS $_3$ Cu $_3(\mu_2$ -I) $_3$ ]} $_n$  shows self-defocusing behavior and {[NMe $_4$ ] $_2$ [WOS $_3$ Cu $_3(\mu_2$ -I) $_3$ ]} $_n$  shows self-focusing effects.<sup>28</sup> However, the NLO properties of the title complexes **1** and **2** are switched from NLO absorption to NLO refraction.

**Acknowledgment.** We thank the National Natural Science Foundation of China (Nos. 2001006 and 20371042), the Excellent Young Teachers Program In Higher Education Institute, and Henan Province for support.

**Supporting Information Available:** Crystallographic data for **1** and **2** in CIF format. This material is available free of charge via the Internet at <http://pubs.acs.org>.

IC035244+

(23) (a) Wang, Y.; Cheng, L. *J. Phys. Chem.* **1992**, *96*, 1530. (b) Guha, S.; Frazier, C. C.; Porter, P. L.; Kang, K.; Finberg, S. *Opt. Lett.* **1989**, *14*, 952. (c) Ghosal, S.; Samoc, M.; Prasad, P. N.; Tufariello, J. J. *J. Phys. Chem.* **1990**, *94*, 2847. (d) Guha, S.; Frazier, C. C.; Porter, P. L.; Kang, K.; Finberg, S. E. *Opt. Lett.* **1989**, *14*, 952. (e) Blau, W. J.; Byrne, H. J.; Cardin, D. J.; Davey, A. P. *J. Mater. Chem.* **1991**, *1*, 245. (f) Hou, H. W.; Meng, X. R.; Song, Y. L.; Fan, Y. T.; Zhu, Y.; Lu, H. J.; Du, C. X.; Shao, W. H. *Inorg. Chem.* **2002**, *41*, 4068.

(24) Ge, P.; Tang, S. H.; Ji, W.; Shi, S.; Hou, H. W.; Long, D. L.; Xin, X. Q.; Lu, S. F.; Wu, Q. J. *J. Phys. Chem. B* **1997**, *101*, 27.  
 (25) Shi, S.; Chen, Z. R.; Hou, H. W.; Xin, X. Q.; Yu, K. B. *Chem. Mater.* **1995**, *7*, 1519.  
 (26) Chen, Z. R.; Hou, H. W.; Xin, X. Q.; Yu, K. B.; Shi, S. *J. Phys. Chem.* **1995**, *99*, 8717.  
 (27) Hou, H. W.; Liang, B.; Xin, X. Q.; Yu, K. B.; Ge, P.; Ji, W.; Shi, S. *J. Chem. Soc., Faraday Trans.* **1996**, *92*, 2343.  
 (28) Hou, H. W.; Wei, Y. L.; Song, Y. L.; Fan, Y. T.; Zhu, Y. *Inorg. Chim. Acta* **2003**, *357*, 421.